MOLECULAR AND CELLULAR BIOLOGY, Sept. 2002, p. 6131–6141 Vol. 22, No. 17
0270-7306/02/$04.00+0 DOI: 10.1128/MCB.22.17.6131–6141.2002

A Gain-of-Function Mutation in the Second Tetratricopeptide Repeat of TFIIIC131 Relieves Autoinhibition of Brf1 Binding

Robyn D. Moir, Karen V. Puglia, and Ian M. Willis*

Department of Biochemistry, Albert Einstein College of Medicine, Bronx, New York 10461

Received 26 March 2002/Returned for modification 7 May 2002/Accepted 4 June 2002

The interaction between the tetratricopeptide repeat (TPR)-containing subunit of TFIIIC, TFIIIC131, and the TFIIB-related factor Brf1 represents a limiting step in the assembly of the RNA polymerase III (pol III) initiation factor TFIIIB. This assembly reaction is facilitated by dominant mutations that map in and around TPR2. Structural modeling of TPR1 to TPR3 from TFIIIC131 shows that one such mutation, *PCF1-2*, alters a residue in the ligand-binding groove of the TPR superhelix whereas another mutation, *PCF1-1*, changes a surface-accessible residue on the back side of the TPR superhelix. In this work, we show that the *PCF1-1* mutation (H190Y) increases the binding affinity for Brf1, but does not affect the binding affinity for Bdp1, in the TFIIIC-dependent assembly of TFIIIB. Interestingly, binding studies with TFIIIC131 fragments indicate that Brf1 does not interact directly at the site of the *PCF1-1* mutation. Rather, the data suggest that the mutation overcomes the previously documented autoinhibition of Brf1 binding. These findings together with the results from site-directed mutagenesis support the hypothesis that gain-of-function mutations at amino acid 190 in TPR2 stabilize an alternative conformation of TFIIIC131 that promotes its interaction with Brf1.

The tetratricopeptide repeat (TPR)-containing subunit of the RNA polymerase III (pol III) assembly factor TFIIIC is conserved from yeasts to humans (7, 13, 32) and plays a central role in recruiting the initiation factor TFIIIB to the DNA upstream of the transcription start site of 5S RNA, tRNA, and other pol III genes with related promoter structures (10, 33, 40). In *Saccharomyces cerevisiae*, the TPR-containing subunit of TFIIIC is a 131-kDa protein known as TFIIIC131 or τ131 (30). TFIIIC131 is the only subunit of TFIIIC that can be photo-cross-linked to DNA within the TFIIIB binding site (2), and its accessibility to photoprobes changes with the stepwise assembly of the preinitiation complex (18, 20). Protein-protein interactions between TFIIIC131 and the TFIIB-related subunit of TFIIIB, Brf1, initially enable only inefficient photo-cross-linking of TFIIIC131 to the upstream DNA. The efficiency of this photo-cross-linking increases significantly with the binding of TATA-binding protein (TBP) and formation of the B′-TFIIIC-DNA complex and then is diminished upon recruitment of the third TFIIIB subunit, Bdp1 (previously known as B″ or TFIIIB90). These observations and the ability of TFIIIC to position TFIIIB at various distances upstream of the A block promoter element (16) are thought to reflect a series of conformational changes that occur in TFIIIC131 during preinitiation complex assembly (20). Conformational changes in the subunits of TFIIIB and the underlying DNA also occur during this process and confer high stability on the TFIIIB-DNA complex under a variety of solution conditions (4, 11, 14, 23, 27, 34). Additionally, deformation of the DNA by TFIIIB is thought to contribute to promoter opening by pol III (reference 22 and references therein).

The activity of TFIIIC131 in pol III transcription is limiting both in vivo and in vitro and can be increased by dominant, gain-of-function mutations (42). Ten mutations of this type have been isolated by using a selection for suppressors of a promoter defect (A19) in the dimeric tRNA gene *sup9-e A19-supS1* (33). These mutations map to a region of approximately 50 amino acids encompassing the second of 11 TPRs in TFIIIC131. The *PCF1-1* mutation was the first of these dominant alleles to be isolated and has one of the strongest suppressor phenotypes in this group (33, 42). Early biochemical studies of the effect of the *PCF1-1* mutation indicated that its ability to increase transcription was correlated with an increase in the activity of fractions containing TFIIIB (35, 41). This resulted from the preferential recovery of Brf1 in TFIIIB fractions from mutant cell extracts (33, 35). Subsequent studies of another TPR2 mutation, *PCF1-2*, employing entirely recombinant TFIIIB, showed that it increased transcription by facilitating the recruitment of Brf1 to TFIIIC-DNA (33). Under the solution conditions employed in this study, transcription and complex assembly with wild-type TFIIIC could not be driven to the same upper limit as was achieved with *PCF1-2* TFIIIC. These data led to the proposal that the mutation facilitated a conformational change in TFIIIC131 that enabled Brf1 binding.

Since the initial genetic and biochemical characterization of *PCF1-1* and *PCF1-2*, several high-resolution structures have been solved for functionally unrelated TPR proteins (1, 5, 9, 26, 37, 39). Each 34-amino-acid-long TPR comprises a pair of antiparallel α helices (designated A and B) connected by a short turn. The similar packing of the helices within and between adjacent tandemly arranged TPRs generates a right-handed superhelix with a groove containing mostly side chains from the A helix. As demonstrated in several TPR-peptide cocrystal structures, the TPR groove provides or supports the ligand-binding surface (9, 26, 37). The *PCF1-2* (T167I) and *PCF1-1* (H190Y) mutations change residues in the A and B helices, respectively, that are not part of the consensus that

* Corresponding author. Mailing address: Department of Biochemistry, Albert Einstein College of Medicine, 1300 Morris Park Ave., Bronx, NY 10461. Phone: (718) 430-2839. Fax: (718) 430-8565. E-mail: willis@aecom.yu.edu.

defines the TPR fold (5). Thus, the different locations of these mutations suggest that they may activate pol III gene transcription by different mechanisms. In addition, studies showing that TFIIIC131 plays a role in the recruitment of Bdp1 and interacts directly with this factor suggest an alternative step in TFIIIB complex assembly (other than Brf1 binding) that might be targeted by dominant *PCF1* alleles (7, 36).

The interaction between TFIIIC131 and Brf1 has been demonstrated in two-hybrid experiments (3), in pull-down assays (24), and in solution interaction assays where it has been shown to proceed with the acquisition of α helicity in one or both proteins (31). The amino-terminal half of TFIIIC131 contains two independent binding sites for Brf1: a high-affinity site in the amino terminus up to TPR5 (Nt-TPR5) and a lower-affinity site in TPR6 to TPR9. Interestingly, a larger fragment (Nt-TPR9) containing both of these sites has significantly lower affinity for Brf1 than either of the two smaller fragments. These findings demonstrate that autoinhibition of Brf1 binding sites in TFIIIC131 limits the interaction between these components in vitro. However, evidence that this phenomenon is biologically relevant for TFIIIC131 function has not yet been reported.

In this work, we have examined the mechanism of activation by *PCF1-1*. We show that the mutation (H190Y) increases the affinity of the interaction between TFIIIC-DNA and Brf1. However, site-directed mutagenesis experiments and binding studies with fragments of TFIIIC131 suggest that Brf1 does not make a direct contact with the side chain at amino acid 190 in TFIIIC131. Instead, dominant mutations at this position are shown to overcome the previously observed autoinhibition in the Brf1 binding reaction. The molecular basis of this effect is suggested to involve the stabilization of an intramolecular interaction in TFIIIC131 that promotes the interaction with Brf1.

MATERIALS AND METHODS

Generation and analysis of site-directed mutations. The Morph S site-specific plasmid DNA mutagenesis kit (5 Prime→3 Prime, Boulder, Colo.) was used per the manufacturer's directions. Degenerate oligonucleotides with the sequence CCTGGCAGCTXXXCTAAATGCATCCGATTGGG were used to mutagenize the plasmid pRS313*PCF1*$^+$ at codon 190. Mutant plasmids were identified by the acquisition of an *Nsi*I restriction site (underlined) introduced by silent mutagenesis. Candidate clones were retransformed into DH5α, rescreened by *Nsi*1 digestion, and sequenced to confirm the identity of the amino acid substitution. *PCF1* alleles on pRS313 were transformed into the yeast strain supAC1+ (see below), and the rescuing plasmid (pRS316*PCF1*$^+$) was evicted on medium containing 5-fluoroorotic acid. Single colonies were obtained and assayed for viability and *supS1* suppressor activity at 16, 30, and 37°C.

Molecular modeling. Deep View software version 3.7b2 (12) was used to construct a model of TPR1 to TPR3 from TFIIIC131 based on the structure of protein phosphatase 5 (PP5 [5]). Deep View aligned the TPRs of the two proteins without any discontinuity and then threaded the sequence from TFIIIC131 onto the TPR structure of PP5 to generate the initial model. Subsequent energy minimization was performed with the GROMOS96 implementation in Deep View. Statistical analysis of structural models was performed with WHAT_CHECK software (http://www.cmbi.kun.nl: 1100/WIWWWI).

Proteins. The purification of recombinant TFIIIB subunits (Brf1, TBP, and Bdp1) and yeast TFIIIC fractions has been described previously (4, 28, 31, 33). The specific activity of Brf1 in supporting single-round transcription was measured as described previously (28). For TFIIIC, whole-cell extracts from the *S. cerevisiae* strains supAC1+ (MATα *ura3-52 pcf1*Δ*::LEU2 his3-11,15 leu2-3,112 trp1-1 met8-1 lys2*Δ*::sup9eA19-supS1* pRS316 *PCF1*+) and supAC1-1 (same as supAC1+ but substituting pRS316 *PCF1-1* [35]) were purified over four chromatographic columns (19, 23). Briefly, this involved step elution from BioRex70 and DEAE-Sephadex A25 and gradient elution from heparin-agarose and MonoQ columns. The resulting TFIIIC fractions had comparable DNA binding activities and generated apparent dissociation constants of 1.6×10^{-10} and 2.2×10^{-10} M for *PCF1*$^+$ and *PCF1-1*, respectively. Western analysis for TFIIIC131 confirmed that the yield of TFIIIC was unaffected by the H190Y mutation (data not shown). Recombinant fragments of TFIIIC131 carrying the H190Y substitution were cloned, expressed, and purified as described elsewhere for their wild-type counterparts (32).

Two-hybrid assays. Interactions were assayed with Brf1 and Bdp1 in pASCHY2 and wild-type or mutant TFIIIC131 in pACTII (8). The reciprocal interactions between Brf1 in pACTII and TFIIIC131 in pASCHY2 were also measured. The resulting β-galactosidase activity (units per milligram of protein) in the haploid yeast strain Y190 was measured after glass bead breakage (3, 8). Control experiments showed no β-galactosidase activity, above that of the vector alone, in the absence of a partner protein.

Complex assembly assays. Complex assembly and electrophoresis on native polyacrylamide gels were performed with only minor modifications to previously described methods (31, 32). Unless otherwise indicated, reaction mixtures contained *sup3-eST* labeled DNA (10 fmol), yeast TFIIIC (5 fmol), Brf1 (6,000 fmol), TBP (250 fmol), and Bdp1 (100 fmol) with duplex poly(dG-dC) (25 μg/ml) as a nonspecific competitor DNA. For all experiments, TFIIIC-DNA complexes were preformed (20°C for 10 min) prior to addition of the other components. Reaction mixtures were then incubated at 20°C for an additional 60 min. In Fig. 3 to 5, duplex poly(dI-dC) (25 μg/ml) was used in place of duplex poly(dG-dC) to titrate trace amounts of TBP in the TFIIIC fractions or to limit the TBP concentration in the assembly of B′-TFIIIC-DNA complexes. The recruitment of Brf1 to mutant and wild-type TFIIIC-DNA complexes was examined in parallel experiments over a range of Brf1 concentrations from 25 to 900 nM. To assess the stability of Brf1-TFIIIC-DNA during electrophoresis, wild-type complexes were assembled and electrophoresed for 1, 2, 3, and 4 h. For Bdp1 titration experiments, template DNA (4 fmol), TFIIIC (0.3 to 2.5 fmol), Brf1 (6,000 fmol), and either 20 or 200 fmol of TBP were used to generate the substrate complex (B′-TFIIIC-DNA) for Bdp1 binding. The latter level of TBP drives higher-order complex formation essentially to completion with poly(dG-dC) as the nonspecific DNA. The recruitment of Bdp1 to mutant and wild-type complexes was examined in parallel over a range of concentrations from 0.5 to 20 nM. The ability of fragments of TFIIIC131 to bind to Brf1 in solution and thus inhibit TFIIIB-DNA complex formation was determined as previously described (31, 32). TFIIIC131 fragments were added to preformed TFIIIC-DNA complexes prior to the addition of the TFIIIB subunits. Mutant and wild-type fragments were always assayed in parallel. Individual pairwise comparisons (wild-type versus mutant) of inhibition isotherms generated with Nt-TPR9 and TPR1 to TPR9 always returned a higher apparent affinity (approximately twofold) for the mutant fragment. In contrast, individual experiments with mutant and wild-type Nt-TPR5 and TPR1-to-TPR5 fragments always generated inhibition isotherms that were identical within experimental error.

Quantitation and data analysis. TFIIIB complex formation was quantified and analyzed as described previously (32). Briefly, digital images collected on phosphor storage screens were quantified with ImageQuant software. Individual lines, one lane wide, were analyzed by using Peak Finder to calculate peak areas corresponding to the TFIIIB-TFIIIC-DNA or heparin-stripped TFIIIB-DNA complexes. These values, when paired with the appropriate concentration of either Bdp1 or TFIIIC131 fragment, yielded a transition curve describing the formation or inhibition of complex assembly, respectively. For Bdp1 incorporation into TFIIIB complexes, the substrate concentration (B′-TFIIIC-DNA) was determined to be less than 20 pM, which is >50-fold lower than the apparent equilibrium dissociation constant determined for Bdp1 binding (see Results). Thus, under the conditions employed, the difference between the total and free Bdp1 concentrations in the reactions is negligible. The upper limit of complex assembly was determined by nonlinear least squares analysis with the Hill equation and Microcal Origin version 5.0 software (Microcal Software Inc.) This limiting value was used to generate a scaled isotherm in which the relative level of TFIIIB-DNA complex formation is expressed as a function of either Bdp1 or TFIIIC131 fragment concentration. Multiple scaled data sets generated with either wild-type or mutant TFIIIC were then refitted to the Hill equation. Errors associated with the apparent equilibrium dissociation constants and the Hill coefficients were determined during curve fitting.

To quantify the incorporation of Brf1 into TFIIIC-DNA complexes, the widths of the lines used for Peak Finder were set to exclude the edges of each lane (where peak trailing compromises band resolution). The curves generated by Peak Finder were then analyzed with the Peak Fitting software in Microcal Origin version 5.0, as follows. The curve parameters that best described the TFIIIC-DNA band were determined for the wild-type and mutant TFIIIC frac-

tion in each experiment. In addition, the physical separation of TFIIIC-DNA and Brf1-TFIIIC-DNA complexes was determined from a lane in each titration where the band intensities of the two species were approximately equal. These parameters were used to define the shape and peak position of the two complexes for each lane in the corresponding Brf1 titration experiment. Two individual curves were then fitted for each curve generated by Peak Finder until the error was minimized. Brf1-TFIIIC-DNA complex formation, calculated as the fraction of the total number of TFIIIC-DNA complexes, was analyzed as described above. The quantitation of Brf1-TFIIIC-DNA complexes required that both TFIIIC-DNA and Brf1-TFIIIC-DNA bands be symmetrical (neither complex formed a trailing edge in the gel) and that no lane distortion occur during gel electrophoresis or drying.

RESULTS

Substitutions at amino acid 190 in TPR2 of TFIIIC131 increase or decrease expression of *sup9-e A19-supS1*. To gain some structural insight into the activating function of the *PCF1-1* mutation, we threaded the sequence of TPR1 to TPR3 from TFIIIC131 (102 amino acids) onto the structure of the three TPRs of PP5 with Deep View software (version 3.7b2). The computer-generated alignment contained no gaps and correctly positioned the TPRs of TFIIIC131 with those of PP5 (which are 19% identical in sequence). The structural model obtained after energy minimization contained no amino acid side chain or backbone clashes. Statistical evaluation of the model showed it to be similar in overall quality to the PP5 template despite some relaxation of side chain planarity and dihedral angle distribution. In the model (Fig. 1), the tyrosine residue resulting from the *PCF1-1* mutation at amino acid 190 has been introduced and its position is shown in relation to amino acid 167, site of the *PCF1-2* mutation. The side chain of amino acid 190 does not influence the packing of the TPR helices and, unlike amino acid 167, does not project into the ligand-binding groove. Rather, residue 190 is surface accessible on the back side of the TPR superhelix. As such, it is a likely site for intra- or intermolecular interactions.

If the *PCF1-1* mutation were to enable a novel interaction, relatively few amino acids would be predicted to exhibit the mutant behavior. However, if the mutation disrupted an inhibitory interaction (thereby promoting TFIIIB complex assembly), a wide variety of mutations at this site might have the same phenotype. A phylogenetic analysis supports the former possibility, since amino acid 190 of TFIIIC131 is highly conserved from yeasts to humans (7, 32). To further examine this issue, we conducted site-directed mutagenesis to test the effect of changes at this position on the growth of *S. cerevisiae* on complete medium and the ability to suppress the *sup9-e A19* promoter defect (see Materials and Methods). Eleven *PCF1* alleles were constructed. These alleles, together with *PCF1-1* and the wild-type gene, were plasmid shuffled into strain supAC1, which has the chromosomal *PCF1* gene deleted and contains the *sup9-e A19-supS1* reporter. Eviction of the rescuing *URA3*-marked *PCF1*$^+$ plasmid showed that none of the H190 substitutions conferred a lethal or conditional growth phenotype at 16, 30, or 37°C on complete medium (Fig. 2 and data not shown). In screening for increased pol III transcription of the *sup9-e A19-supS1* reporter (Fig. 2), four substitutions (Phe, Leu, Trp, and Ile) were identified that had *supS1* suppressor activities intermediate between those of *PCF1-1* (Tyr) and wild type (His). Interestingly, seven other substitutions (Ala, Asn, Gly, Arg, Ser, Pro, and Gln) resulted in a weaker suppressor phenotype than the wild type. These data indicate that, although a wide variety of substitutions can be tolerated at position 190, small hydrophobic (Ala) or polar (Ser, Asn, and Gln) residues, a basic residue (Arg), and helix-breaking-destabilizing (Pro and Gly) residues do not support normal function as well as does the wild-type (His) residue. Moreover, the wild-type residue appears to have been selected through evolution to have an intermediate level of activity. This activity can be increased by substitutions with aromatic (Tyr, Trp, and Phe) or large hydrophobic (Ile and Leu) residues. Thus, the dominant mutations at position 190 are hypermorphic alleles: they increase the function relative to the wild type by enhancing an interaction at this site. Importantly, these results do not distinguish between a direct and an indirect effect of these mutations on ligand binding. However, the experiments reported below support an indirect mechanism of action.

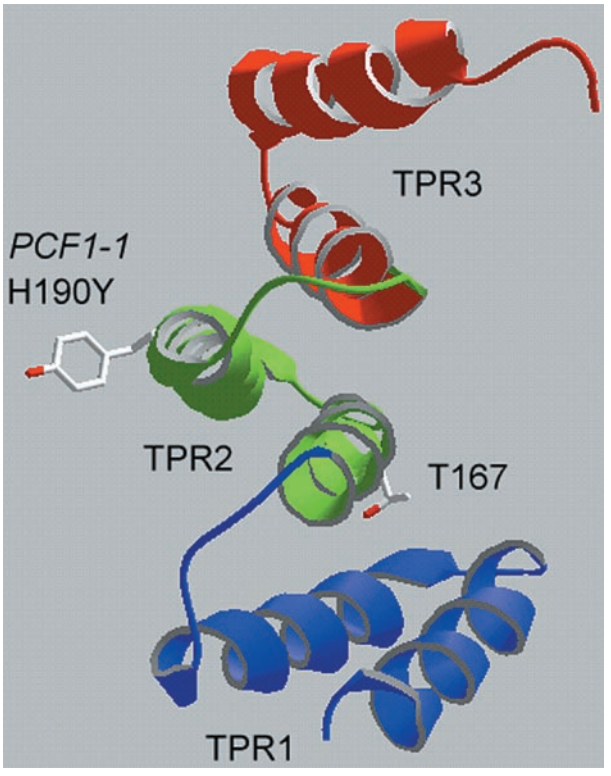

FIG. 1. Structural model of TPR1 to TPR3 of TFIIIC131. The model was generated by using Deep View software and the crystal structure of PP5 (5). The surface accessibility and position of the *PCF1-1* substitution (H190Y) on the back side of the TPR superhelix are shown relative to amino acid 167, site of the *PCF1-2* mutation, which projects into the superhelical groove.

The *PCF1-1* mutation facilitates recruitment of Brf1 to TFIIIC-DNA. Previous biochemical studies of the effects of the *PCF1-2* mutation have shown that it facilitates the recruitment of Brf1 to TFIIIC-DNA and thereby increases the number of TFIIIB-TFIIIC-DNA complexes (33). The *PCF1-2* mutation is located in the A helix of TPR2 and changes a residue that projects into the ligand-binding groove of the TPR superhelix (Fig. 1) (5, 33). Given the different locations of the *PCF1-1* and *PCF1-2* mutations in the TPR structure, different mechanisms

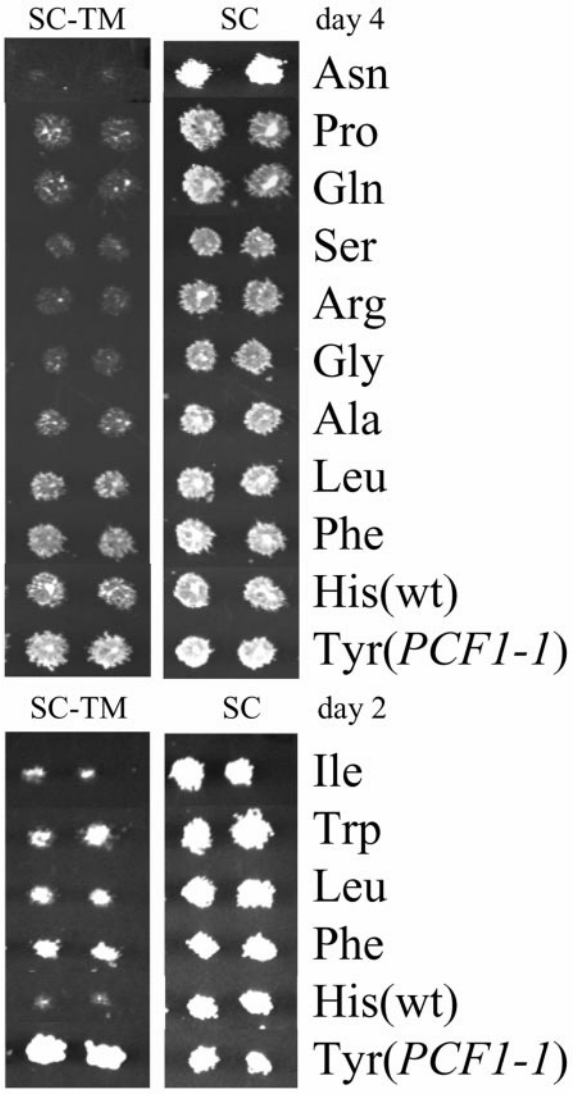

FIG. 2. Suppressor phenotypes of mutations at amino acid 190 of TFIIIC131. The suppressor phenotype of two individual isolates of each new *PCF1* allele, in strain supAC1+, is shown in the upper left panel (grown on synthetic complete medium without tryptophan or methionine for 4 days at 30°C). The suppressor phenotype of the gain-of-function *PCF1* alleles is shown in the lower left panel (grown for 2 days at 30°C). The corresponding growth phenotype on complete medium is shown in the right panels (grown for 4 and 2 days at 30°C, upper right and lower right panels, respectively). Note the difference in suppressor phenotype (colony size) of His (wild type) between 2 and 4 days of growth. The *PCF1-1* (Tyr) allele shows a robust suppressor phenotype at 2 days and earlier.

might underlie their ability to increase pol III transcription. To begin to address this possibility, we have compared the specific activities of TFIIIC fractions purified from wild-type and *PCF1-1* strains in the assembly of recombinant TFIIIB subunits onto DNA. For these experiments, TFIIIC from wild-type and *PCF1-1* whole-cell extracts was purified over four chromatographic columns. The factor from each extract was obtained in similar yield as judged by Western blotting with antibodies to the 95-, 131-, and 138-kDa subunits (data not shown) and had equivalent DNA binding affinity for a tRNA gene probe (K_{app}, 2.2×10^{-10} and 1.6×10^{-10} M for *PCF1-1* and wild-type TFIIIC, respectively).

To quantify the assembly of TFIIIC-DNA and higher-order complexes, reactions at equilibrium were resolved on native polyacrylamide gels. Equal numbers of *PCF1-1* and wild-type TFIIIC-DNA complexes were assembled based on the empirically determined DNA binding activities (Fig. 3, lanes 1 and 2). With the addition of a subsaturating amount of Brf1 (6,000 fmol), the mutant TFIIIC forms twofold more of the Brf1-TFIIIC-DNA complex than does wild-type TFIIIC (compare lanes 3 and 4). Consistent with this, it takes twice the amount of Brf1 (12,000 fmol) to generate similar levels of Brf1-TFIIIC-DNA complexes on wild-type TFIIIC as with mutant TFIIIC-DNA (lanes 4 and 5). Similar results are seen in the assembly of B′-TFIIIC-DNA (lanes 6 to 8), although the inability to resolve all of the complexes precludes their quantitation. Nonetheless, it is apparent that increasing the amount of Brf1 drives the assembly of higher-order complexes and diminishes the amount of wild-type TFIIIC-DNA (lanes 6 and 8). Differential binding of Brf1 to *PCF1-1* and wild-type TFIIIC is also reflected in the number of TFIIIB-TFIIIC-DNA complexes (lanes 9 and 10) and heparin-resistant TFIIIB-DNA complexes (lanes 12 and 13). As will become apparent in later experiments, this in vitro differential in TFIIIB complex assembly is observed only under conditions where both Brf1 and TBP are limiting. That TBP is limiting under the conditions used in Fig. 3 is shown by the ability of additional TBP, but not Brf1 or Bdp1, to drive higher levels of TFIIIB-TFIIIC-DNA complex assembly with wild-type TFIIIC (compare lanes 11, 14, and 15 with lane 9). Additional Brf1 increases the level of Brf1-TFIIIC-DNA complexes (compare lanes 9 and 11), which accumulate rather than being converted into TFIIIB owing to the limited amount of TBP. Under these conditions, the addition of extra Bdp1 does not generate an increase in TFIIIB-TFIIIC-DNA complexes (compare lanes 9 and 15). It is, therefore, the addition of TBP in lane 14 that allows the assembly of higher levels of TFIIIB-TFIIIC-DNA complexes with wild-type TFIIIC (compare lane 9 to lane 14) and thus mimics the effect of the *PCF1-1* mutation. Thus, as observed previously for the *PCF1-2* mutation (33), *PCF1-1* facilitates the recruitment of Brf1 to TFIIIC-DNA and allows the assembly of more TFIIIB complexes under conditions where both Brf1 and TBP are limiting.

Determination of an apparent binding affinity for the interaction of Brf1 with TFIIIC-DNA. Although the *PCF1-1* mutation does not map to a TPR position that is known from structural studies to participate directly in ligand binding, the effect of the mutation on ligand (Brf1) binding affinity, be it direct or indirect, has not been assessed to date. Indeed, the affinity of Brf1 for wild-type TFIIIC-DNA has not yet been determined. In this regard, the relatively small amounts of TFIIIC that are available and the high nonspecific binding of Brf1 to solid supports (28) pose significant obstacles for a variety of quantitative methods. We, therefore, explored the feasibility of directly quantifying the interaction between TFIIIC-DNA and Brf1 by native gel electrophoresis. Owing to the limited separation of TFIIIC-DNA and Brf1-TFIIIC-DNA complexes, several modifications to our protocol for quantifying TFIIIB-DNA complexes (31, 32) were necessary in order to obtain binding curves from these experiments (see Materials

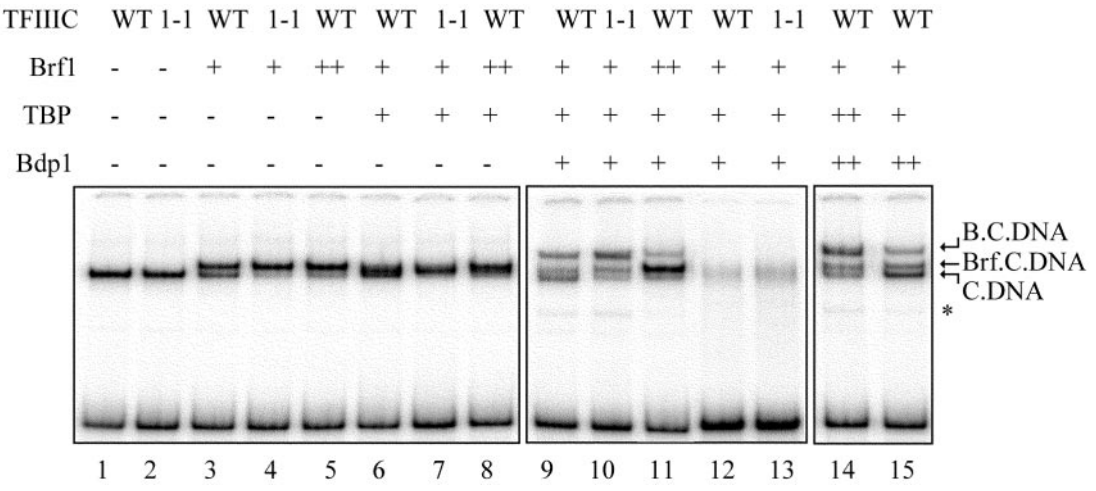

FIG. 3. Complex assembly by wild-type and *PCF1-1* TFIIIC. Wild-type (WT) or *PCF1-1* (1-1) TFIIIC-DNA complexes were preassembled for 10 min on a ^{32}P-labeled *sup3-eST* tRNA gene prior to the addition of subsaturating levels of Brf1 (6,000 fmol) or TBP [250 fmol; note that poly(dI-dC) was used in these reactions; see Materials and Methods] and saturating levels of Bdp1 (100 fmol) as indicated above each lane; ++ indicates that twice the above amount of the specified factor was used. After complex assembly for 60 min at 20°C, samples were resolved on a native 4% polyacrylamide gel. Reaction mixtures in lanes 12 and 13 were challenged with heparin (300 μg/ml) before loading to compare the number of TFIIIB-DNA complexes (TFIIIC-DNA, Brf1-TFIIIC-DNA, and TBP-Brf1-TFIIIC-DNA complexes do not survive heparin treatment [25]). Note that the recruitment of TBP to Brf-TFIIIC-DNA complexes (lanes 7 and 8) generates a complex on the *sup3-e* tRNA gene that migrates faster than the Brf1-TFIIIC-DNA complex. The asterisk marks TATA-directed, TFIIIC-independent, TFIIIB-DNA complex formation, ~2% of the TFIIIB-TFIIIC-DNA complexes assembled in this assay.

and Methods). Most importantly, only gels of the highest quality (in band resolution and uniformity) were analyzed, and we incorporated the use of peak fitting software together with strict criteria for peak shape to quantify each species. As a first test of this approach, Brf1-TFIIIC-DNA complexes were assembled under identical conditions by using wild-type TFIIIC and electrophoresed in a native gel for 1, 2, 3, and 4 h (Fig. 4) (see Materials and Methods). Complexes electrophoresed for 1 h were not resolved sufficiently to allow quantitation of individual species. For the other time points, the formation of Brf1-TFIIIC-DNA was quantified as a fraction of the total number of TFIIIC-containing complexes. This analysis showed no significant variation in the fraction of Brf1-TFIIIC-DNA and yielded an average value of 49% ± 5%. Thus, the complexes appear to be relatively stable during electrophoresis.

The ability of mutant and wild-type TFIIIC-DNA complexes to bind Brf1 was determined by nonlinear least squares analysis (31, 32) after peak fitting (as above) to calculate the fraction of Brf1-TFIIIC-DNA complexes assembled over a range of Brf1 concentrations. Representative titrations of Brf1 on wild-type and mutant TFIIIC-DNA complexes are shown together with their corresponding peak-fitted curves in Fig. 5. The data from this experiment and additional independent experiments were simultaneously fitted to the Hill equation to obtain the binding curves in Fig. 6. In agreement with the results in Fig. 3 (lanes 3 and 4), wild-type TFIIIC is less efficient than mutant TFIIIC in forming Brf1-TFIIIC-DNA complexes at limiting concentrations of Brf1. In addition, wild-type TFIIIC-DNA complexes appear to be limited in the extent to which the Brf1 binding reaction can proceed; approximately 20% of the wild-type TFIIIC-DNA complexes persist at apparently saturating concentrations of Brf1 whereas the mutant TFIIIC-DNA complexes are quantitatively converted into

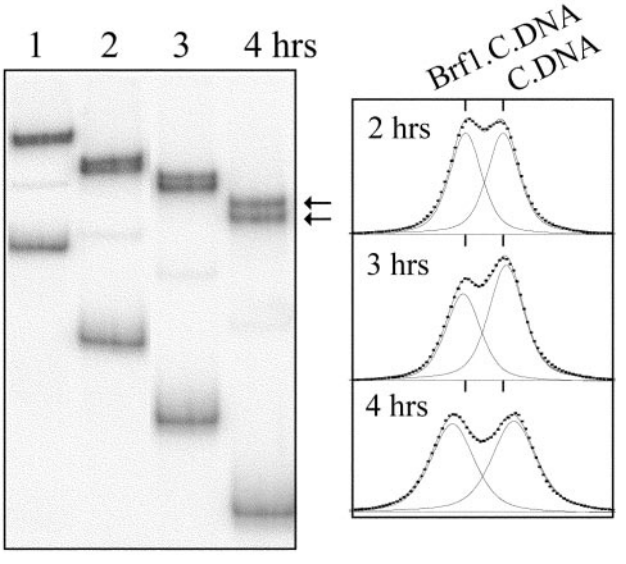

FIG. 4. Stability of Brf1-TFIIIC-DNA complexes during electrophoresis. (Left) Wild-type TFIIIC-DNA complexes were assembled into Brf1-TFIIIC-DNA complexes with subsaturating amounts of Brf1 (6,000 fmol) for 60 min prior to native gel electrophoresis for 1, 2, 3, and 4 h. Arrows indicate the positions of the Brf1-TFIIIC-DNA and TFIIIC-DNA complexes after electrophoresis for 4 h. (Right) Resolution and curve fitting of Brf1-TFIIIC-DNA and TFIIIC-DNA complexes from the left panel. The analysis is shown for complexes electrophoresed for 2, 3, and 4 h. The Peak Finder curve (ImageQuant) that describes the band intensities from the left panel is represented by symbols (squares). The sum of the individual peak fit curves (Microcal Origin) for Brf1-TFIIIC-DNA (left peak) and TFIIIC-DNA (right peak) is represented by a solid line. Note that this line is superimposed on the primary data.

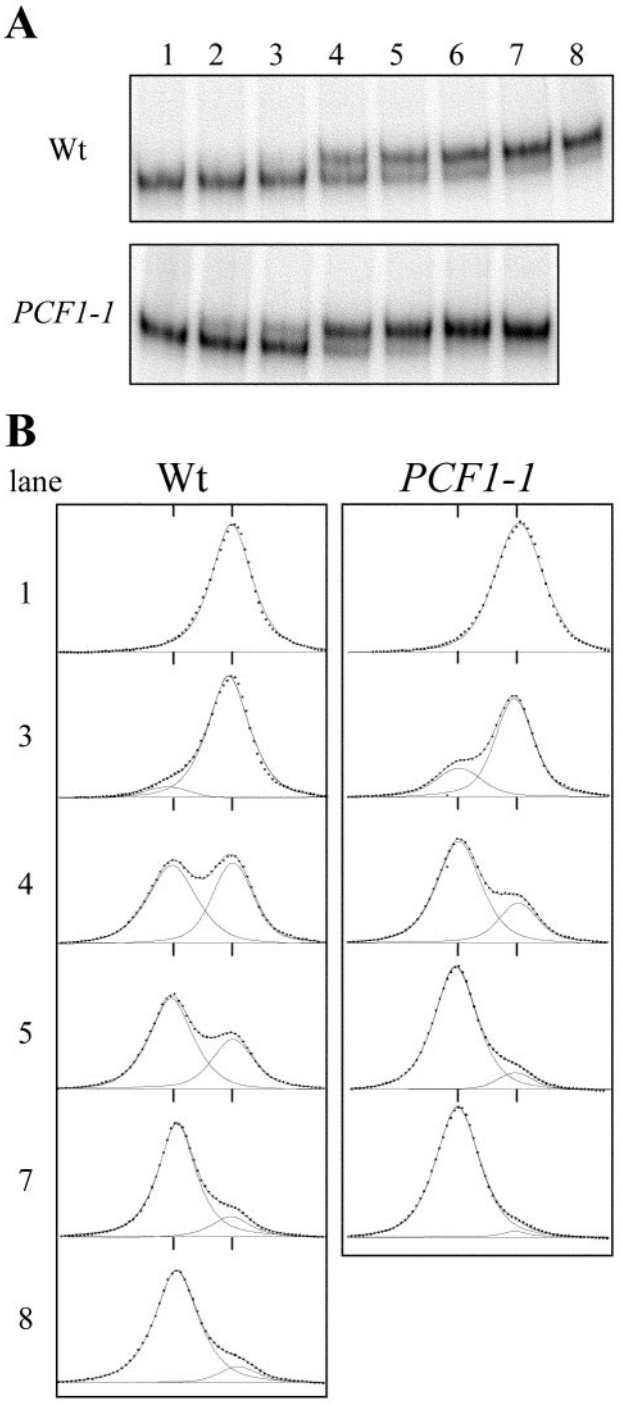

FIG. 5. Titrations of Brf1 on wild-type and *PCF1-1* TFIIIC-DNA complexes. (A) Representative gels of Brf1 titrations with wild-type (upper panel) and *PCF1-1* (lower panel) TFIIIIC. Lanes 1 to 8, 0, 0.5, 1.0, 3.0, 6.0, 9.0, 12.0, and 18.0 pmol of Brf1, respectively. (B) Peak fitting analysis for selected lanes from panel A (corresponding to 1.0, 3.0, 6.0, 12.0, and 18.0 pmol of Brf1). The Peak Finder curve (ImageQuant) is represented by symbols (squares), and the sum of the peak fit curves for Brf1-TFIIIC-DNA (left peak) and TFIIIC-DNA (right peak) is represented by a solid line. Small vertical lines mark the positions of the two peaks used to constrain the peak fitting software (see Materials and Methods). Note that residual wild-type TFIIIC-DNA complexes remain in lane 8 at the highest level of Brf1.

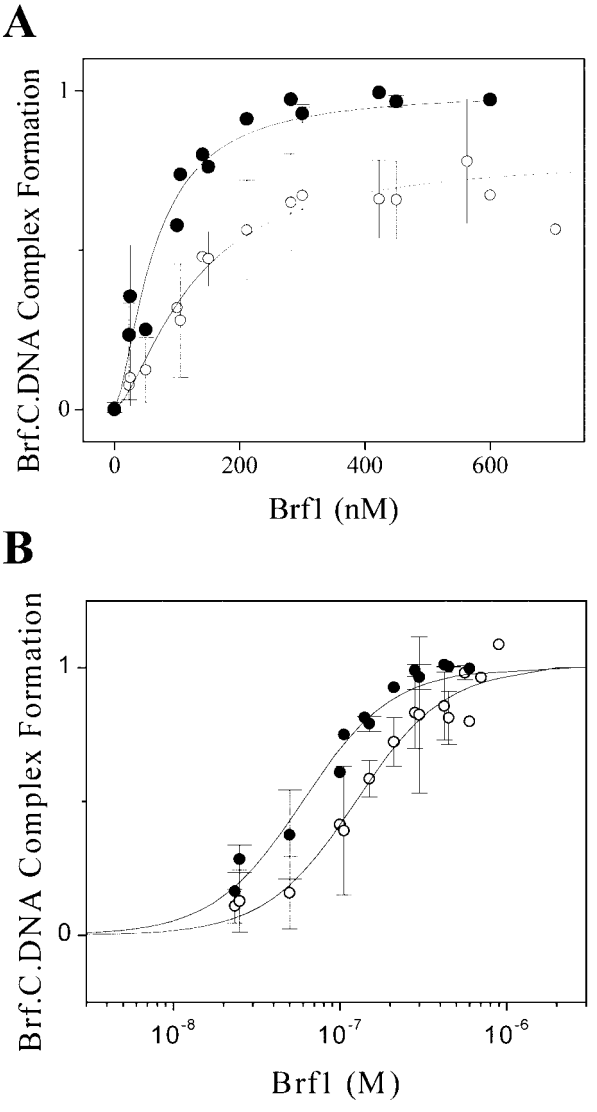

FIG. 6. Apparent affinity of Brf1 for TFIIIC-DNA complexes. (A) For each titration (examples are shown in Fig. 5) Brf1-containing complexes were quantified and expressed relative to an upper endpoint of 1.0 which represents complete conversion of TFIIIC-DNA into Brf1-TFIIIC-DNA (see Materials and Methods). Where replicate data points at a given Brf1 concentration were available, the data were averaged and are plotted with the associated error bars for wild-type TFIIIC (open symbols) and *PCF1-1* TFIIIC (solid symbols). (B) Brf1 titrations (like those in Fig. 5) were individually fitted to define an upper endpoint. The data were scaled to that endpoint and then averaged, where multiple data points were available, to generate a global binding isotherm for Brf1 recruitment on wild-type TFIIIC (open symbols) and *PCF1-1* TFIIIC (solid symbols).

Brf1-TFIIIC-DNA. This behavior was noted previously in our analysis of TFIIIC from wild-type and *PCF1-2* strains (33).

To determine the affinity of TFIIIC-DNA for Brf1, each Brf1 titration was individually fitted to define an upper endpoint, the data were scaled to that endpoint, and then multiple data sets were simultaneously refitted to obtain binding isotherms for the mutant and wild-type factor (Fig. 6B and Materials and Methods). This analysis yielded an apparent affinity for mutant TFIIIC (60 ± 4 nM) that is twofold higher than that

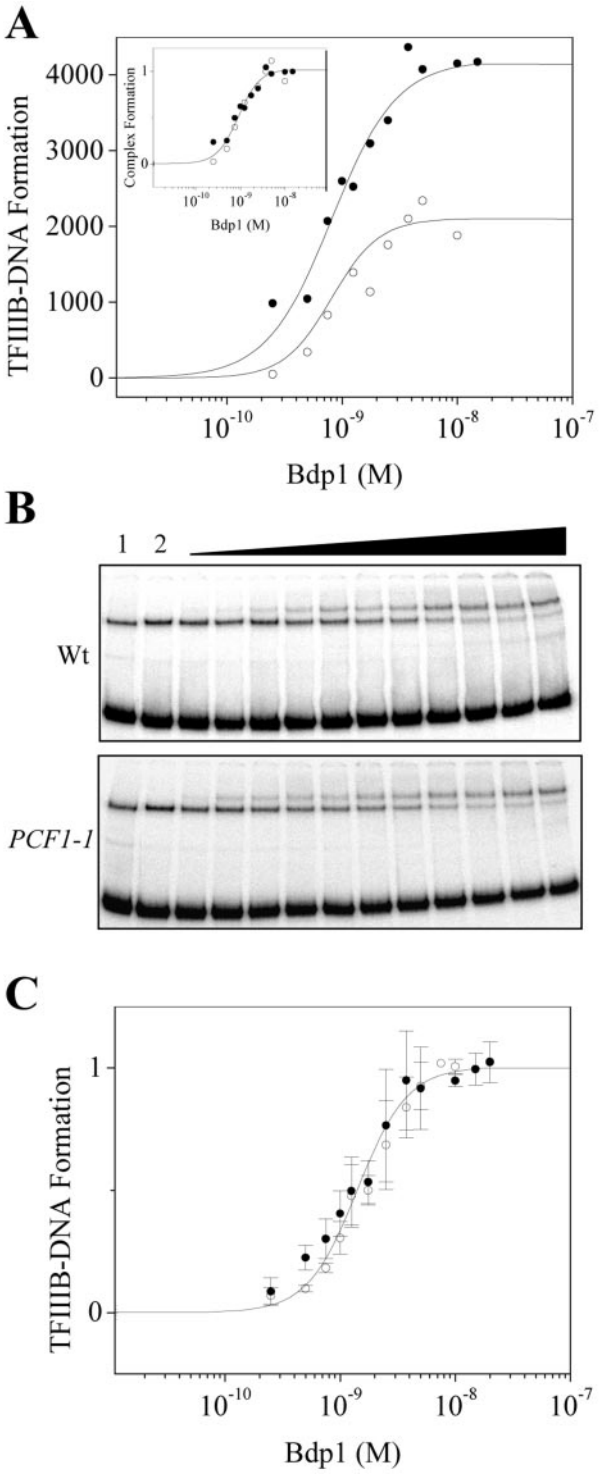

FIG. 7. Recruitment of Bdp1 to B′-TFIIIC-DNA complexes containing wild-type or *PCF1-1* TFIIIC. (A) Binding isotherms for Bdp1 recruitment by B′-TFIIIC-DNA complexes that were assembled with subsaturating amounts of both Brf1 (6,000 fmol) and TBP (20 fmol) with poly(dG-dC) as the nonspecific competitor DNA. These conditions maintain the differential between wild-type TFIIIC (open symbols) and *PCF1-1* TFIIIC (solid symbols) in TFIIIB complex formation (similar to Fig. 3). The isotherms obtained when these data are scaled to their respective endpoints are shown in the inset to panel A. (B) Representative native gels of Bdp1 titrations on B′-TFIIIC-DNA complexes assembled with wild-type (upper panel) or *PCF1-1* (lower panel) TFIIIC. Reaction conditions were the same as for panel A except for TBP (200 fmol), which is saturating for TFIIIB complex assembly under these conditions. Lane 1, TFIIIC-DNA alone; lane 2, B′-TFIIIC-DNA; lanes 3 to 13, B′-TFIIIC-DNA and 5, 10, 15, 20, 25, 35, 50, 75, 100, 200, or 400 fmol of Bdp1, respectively. (C) Bdp1 binding isotherms obtained from a global analysis of multiple data sets (such as in panel B) for both wild-type (open symbols) and *PCF1-1* (solid symbols) TFIIIC.

for wild-type TFIIIC (122 ± 16 nM). Notably, the same values were derived from the unscaled data (in Fig. 6A), indicating that the analysis was not affected by the different fitting procedures. Interestingly, the best fits to the data returned Hill coefficients of 1.7 ± 0.3 and 1.6 ± 0.2 for wild-type and mutant TFIIIC, respectively. This result reveals a positive cooperativity associated with the binding reaction, since there is substantial evidence that the stoichiometry of the reaction is 1:1 (reference 31 and references therein).

Further evidence that the *PCF1-1* mutation facilitates the interaction between TFIIIC131 and Brf1 was obtained by using the yeast two-hybrid system. Interactions between wild-type TFIIIC131 and Brf1 are readily detected in this system by using β-galactosidase activity as the reporter (3). However, the introduction of the *PCF1-1* mutation into the Gal4 activation domain fusion generated a 26 ± 2-fold-higher level of β-galactosidase activity than wild-type TFIIIC131 when assayed against Brf1 fused to the Gal4 DNA binding domain. The reciprocal fusion protein combination showed a 21 ± 5-fold enhancement of the mutant over wild type. Importantly, Gal4 DNA binding domain fusions of either TFIIIC131 (wild type or mutant) or Brf1 did not produce β-galactosidase activity in the absence of the interacting partner (3; data not shown). These data confirm that the *PCF1-1* mutation positively affects the interaction between TFIIIC131 and Brf1.

Analysis of Bdp1 binding to complexes containing *PCF1-1* or wild-type TFIIIC. Deletion of TPR2 (ΔTPR2) from TFIIIC131 confers a temperature-sensitive phenotype in *S. cerevisiae* that is suppressed by overexpression of Bdp1 but not Brf1 or TBP (7). Similarly, the weak two-hybrid interaction between TFIIIC131 and Bdp1 is stimulated by ΔTPR2 (36) while a negative effect of this deletion is seen on the interaction with Brf1 (3). As TFIIIC131 has recently been shown to interact directly with Bdp1 (7), the preceding findings suggest that dominant mutations like *PCF1-1* in TPR2 may affect the recruitment of Bdp1 to the B′-TFIIIC-DNA complex. To address this possibility, we quantified the binding of Bdp1 to wild-type and *PCF1-1* B′-TFIIIC-DNA complexes. Titrations of Bdp1 were performed on B′-TFIIIC-DNA complexes assembled with limiting amounts of Brf1 and TBP to maintain the differential recruitment of Brf1 (as in Fig. 3). The resulting TFIIIB-TFIIIC-DNA complexes, which are well resolved from the other species (e.g., Fig. 3), were quantified, and the data were plotted as a function of Bdp1 concentration. Binding isotherms obtained by nonlinear least squares analysis show that the mutant TFIIIC supports twofold-more TFIIIB complex formation than does wild-type TFIIIC (Fig. 7A). From these initial fits, each titration was scaled to its upper endpoint and then refitted to the Hill equation. As shown in Fig. 7A (inset), the scaled wild-type and mutant isotherms are indis-

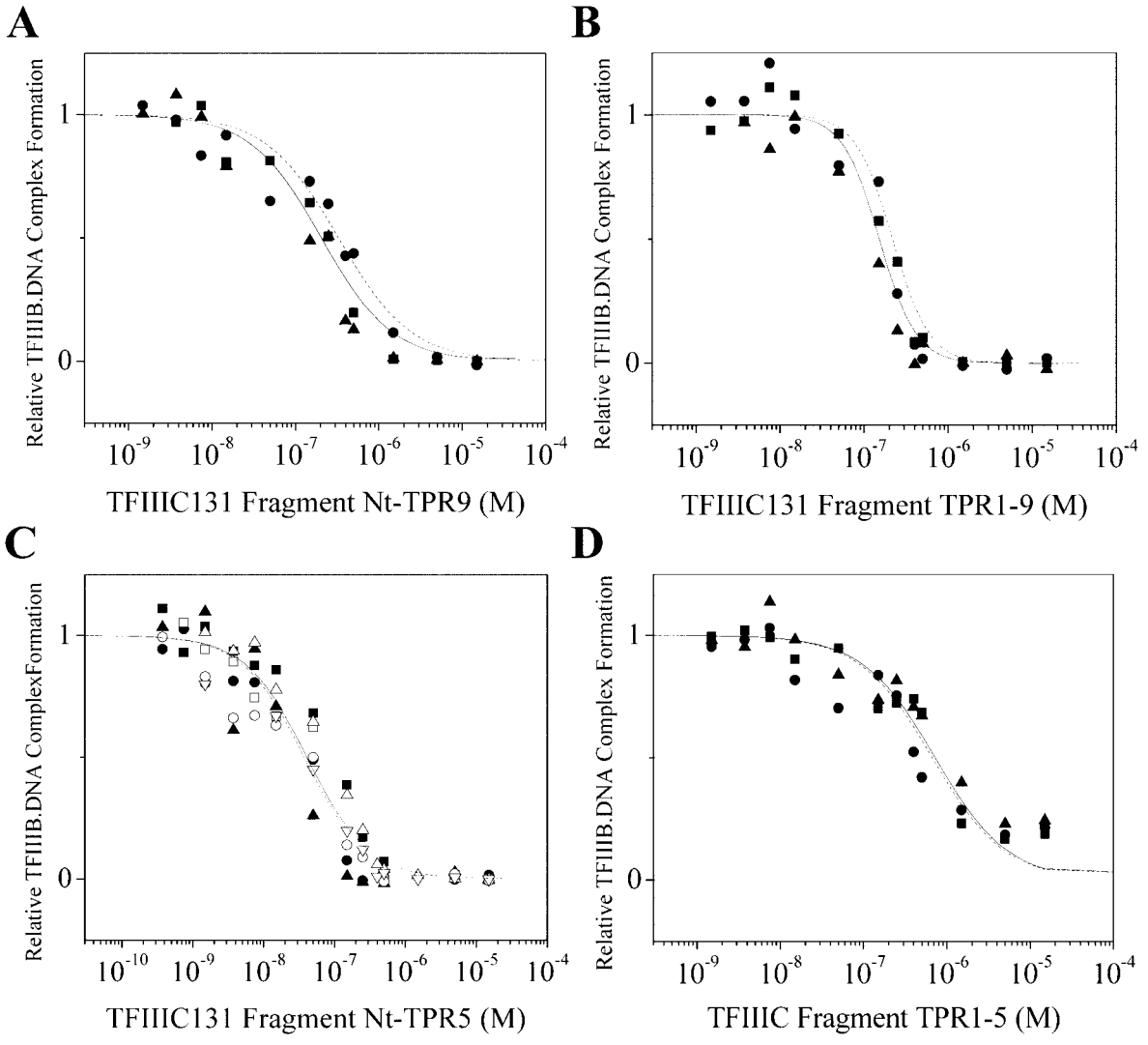

FIG. 8. Inhibition of TFIIIB-DNA complex assembly by fragments of TFIIIC131 containing the *PCF1-1* mutation. TFIIIC131 fragment titrations were performed in a coupled equilibrium binding assay that indirectly monitors the Brf1-fragment interaction in solution (31, 32) (see Materials and Methods). Isotherms describing the inhibition of TFIIIB-DNA complexes by fragments of TFIIIC131 containing the *PCF1-1* mutation (solid line and solid symbols) were determined from a global analysis of multiple data sets (each experiment is represented by a different symbol; see Table 1). Inhibition isotherms generated by the corresponding wild-type fragments are represented only by dashed lines (32). Panels A to D show the effect of the *PCF1-1* mutation in the following fragments of TFIIIC131: Nt-TPR9 (A), TPR1 to TPR9 (B), Nt-TPR5 (C), and TPR1 to TPR5 (D).

tinguishable from one another. We then repeated these Bdp1 titrations in the presence of saturating levels of Brf1 and TBP. In contrast to the limiting conditions used previously, no differential in the level of TFIIIB complex formation was observed for wild-type and mutant TFIIIC under these conditions (Fig. 7B). The resulting binding isotherms demonstrate once again that the *PCF1-1* mutation has no effect on the binding of Bdp1 (Fig. 7C); the wild-type B′-TFIIIC-DNA complex yielded an apparent affinity of 1.65 ± 0.14 nM with a Hill coefficient of 1.7 ± 0.2 whereas the complex containing *PCF1-1* TFIIIC yielded 1.34 ± 0.15 nM with a Hill coefficient of 1.5 ± 0.2. As with the binding of Brf1 to TFIIIC-DNA, the high nonintegral value for the Hill coefficient is indicative of cooperative binding in the recruitment of Bdp1.

We also examined the interaction between full-length Bdp1 and TFIIIC131 by using the yeast two-hybrid system. With TFIIIC131 fused to the Gal4 activation domain, low levels of β-galactosidase activity that were dependent on the DNA binding domain fusion to Bdp1 were obtained for both the wild-type and the mutant protein (4 ± 2 and 1 ± 0.3 U, respectively). Importantly, the *PCF1-1* mutation did not increase the interaction with Bdp1, and therefore, this mutation does not function in a manner analogous to that of a deletion of TPR2 (6, 36).

The *PCF1-1* mutation overcomes autoinhibition of Nt-TPR9 binding to Brf1. Previous biochemical studies have shown that a fragment of TFIIIC131 (Nt-TPR9) encompassing the hydrophilic amino terminus and the two TPR arrays (TPR1 to TPR5 and TPR6 to TPR9 together with the region between them) contains two Brf1 binding sites (32). Each TPR array binds

TABLE 1. Brf1 binding properties of TFIIIC131 proteins containing the *PCF1-1* mutation

Protein	TFIIIC131 (*PCF1*$^+$)[a]		TFIIIC131 H190Y (*PCF1-1*)	
	Global K_D TFIIIB inhibition (nM) ± SE[b]	n^H (Hill coefficient)	Global K_D TFIIIB inhibition (nM) ± SE[b]	n^H (Hill coefficient)
Nt-TPR9	333 ± 21 (6)	−1.3 ± 0.1	192 ± 30 (3)	−1.0 ± 0.2
Nt-TPR5	44 ± 6 (4)	−1.0 ± 0.1	37 ± 8 (3)	−1.1 ± 0.2
TPR1 to TPR9	210 ± 20 (3)	−1.8 ± 0.3	151 ± 16 (3)	−2.1 ± 0.4
TPR1 to TPR5	773 ± 87 (6)	−1.0[c]	722 ± 107 (3)	−1.0[c]

[a] The data for the wild-type fragments were taken from the work of Moir et al. (32).
[b] Errors were determined during curve fitting of multiple concatenated data sets. The number of data sets for each fragment is given in parentheses.
[c] Individual and global fits were performed with the Hill coefficient fixed at 1.0 (as in reference 32).

independently to Brf1, and the inclusion of sequences amino terminal to TPR1 to TPR5 converts this otherwise weak binding fragment into one with high affinity for Brf1 (32). However, the relative Brf1 binding affinities of these fragments indicate that the Nt-TPR5 and TPR6-to-TPR9 sites are not fully accessible to Brf1 within the Nt-TPR9 fragment (32). Thus, the binding of Nt-TPR9 to Brf1 is autoinhibited. These findings suggest that the higher apparent affinity of Brf1 for *PCF1-1* TFIIIC-DNA could be achieved either directly by an enhanced interaction with the TPR1-to-TPR5 binding site or indirectly through the relief of autoinhibition. To examine these possibilities, we assessed the affect of the *PCF1-1* mutation on the Brf1 binding affinity of four TFIIIC131 fragments (Nt-TPR9, Nt-TPR5, TPR1 to TPR5, and TPR1 to TPR9) by a coupled equilibrium binding assay (31, 32). This assay monitors the inhibition of heparin-resistant TFIIIB-DNA complex formation that occurs when TFIIIC131 fragments compete with wild-type TFIIIC-DNA for binding to Brf1 in the presence of excess TBP and Bdp1. Each of the mutant TFIIIC131 fragments was purified to apparent homogeneity as described previously for their wild-type counterparts (32). Titrations of either mutant or wild-type TFIIIC131 fragments were then performed, the heparin-stripped TFIIIB-DNA complexes were resolved in native gels and quantified, and the data were analyzed to extract apparent dissociation constants for the various fragment-Brf1 interactions (32). The wild-type and mutant fragment binding isotherms from these experiments are compared in Fig. 8, and the apparent dissociation constants are listed in Table 1.

The *PCF1-1* mutation has no effect on the low-affinity interaction of Brf1 with TPR1 to TPR5 or its high-affinity interaction with Nt-TPR5. Thus, the interaction of these TFIIIC131 fragments with Brf1 does not involve contacts at amino acid 190. These results are consistent with the idea that the increased binding affinity of Brf1 for mutant TFIIIC-DNA (Fig. 6) is achieved by an indirect mechanism. Further support for this view comes from the positive effect of the *PCF1-1* mutation on Brf1 binding to the Nt-TPR9 and TPR1-to-TPR9 fragments (Table 1). As reported previously (32), autoinhibition of the Brf1 binding sites in Nt-TPR9 is demonstrated by the lower affinity of this TFIIIC131 fragment relative to either Nt-TPR5 or TPR6 to TPR9. Thus, the ability of the *PCF1-1* mutation to increase the affinity of the Brf1-Nt-TPR9 complex without affecting the Brf1–Nt-TPR5 or the Brf1–TPR1-to-TPR5 interactions suggests that the mutation overcomes the autoinhibition seen with the wild-type fragment.

In contrast to the preceding fragments, the mutant and wild-type TPR1-to-TPR9 fragments generate isotherms with Hill coefficients that deviate significantly from unity (Fig. 8 and Table 1). As outlined previously (32), these data suggest two possibilities: that the binding stoichiometry of the reaction has changed such that two molecules of TFIIIB70 are now bound for each molecule of TPR1 to TPR9 or that a single molecule of TFIIIB70 binds cooperatively to the two independent Brf1-binding domains in TPR1 to TPR9. In either case, the apparent affinities of the Brf1–TPR1-to-TPR9 complexes cannot be compared with the affinities of Brf1 complexes involving the other TFIIIC131 fragments. It is clear, however, that the *PCF1-1* mutation increases the affinity of TPR1 to TPR9 for Brf1 (Table 1). For the same reasons as described above for Nt-TPR9, we conclude that the *PCF1-1* mutation opposes the autoinhibition of Brf1 binding to TPR1 to TPR9.

DISCUSSION

The interaction of Brf1 with TFIIIC-DNA complexes represents a limiting step in the recruitment of the transcription initiation factor TFIIIB (29, 33, 38). This step can be facilitated in vivo and in vitro by increasing the amount of Brf1 protein or by increasing the Brf1 recruitment activity of TFIIIC via dominant mutations in TPR1 to TPR3 of TFIIIC131. A structural model of these TPRs in TFIIIC131 (Fig. 1) shows one dominant mutation (*PCF1-2*) projecting into the ligand-binding groove and another (*PCF1-1*) that is surface accessible on the back side of the TPR superhelix. These observations, together with the knowledge that a deletion of TPR2 positively affects the interaction with Bdp1 (36), raised the possibility that different *PCF1* alleles may increase transcription by different mechanisms. In this study we have begun to explore this question by using quantitative biochemical approaches to analyze the effect of the *PCF1-1* mutation on Brf1 and Bdp1 recruitment. We show that the *PCF1-1* mutation increases the apparent binding affinity of Brf1 for TFIIIC-DNA (Fig. 6) while having no discernible effect on the apparent binding affinity of Bdp1 in the final step of TFIIIB complex assembly (Fig. 7). Interestingly, the mechanism by which *PCF1-1* increases Brf1 binding appears not to involve a direct contact with the mutation site. This is demonstrated by the equivalent Brf1 binding affinities of specific wild-type and mutant fragments of TFIIIC131 (Nt-TPR5 and TPR1 to TPR5 [Table 1]). In contrast, the differential affinities (wild type versus mutant) of larger TFIIIC131 fragments that contain part (TPR1 to TPR9) or all (Nt-TPR9) of the two independent Brf1 binding sites support a role for *PCF1-1* in overcoming autoinhibition in the Brf1 binding reaction (32). Autoinhibition of ligand binding

and/or enzymatic activity has also been demonstrated for other well-studied TPR proteins (reference 17 and references therein). Thus, the regulation of autoinhibitory interactions may be a frequently used mechanism to control the functions of this family of proteins.

The preceding findings together with the results from site-directed mutagenesis at amino acid 190 suggest a structural model for activation by dominant, gain-of-function mutations at this position: these mutations, we propose, stabilize an alternative conformation of TFIIIC131 that promotes Brf1 binding. Given the properties of the wild-type and *PCF1-1* fragments of TFIIIC131 (Table 1), the conformer favoring Brf1 binding is predicted to be stabilized by an intramolecular interaction between the tyrosine residue at amino acid 190 and some other site in the Nt-TPR9 fragment. Similar stabilizing interactions are likely for the other activating mutations at this position (Fig. 2). As noted above, a histidine residue at the position corresponding to amino acid 190 in TFIIIC131 is highly conserved in organisms from yeasts to humans and yet has intermediate phenotypic strength. Consistent with the above proposition, this residue presumably has a diminished ability to stabilize the alternative conformer. The biochemical reason that a restrained interaction is preferred is not clear. However, we speculate that the reversible or dynamic nature of the proposed alternative conformer is important for other functions of TFIIIC131. In support of this idea, we note that a specific internal deletion of *BDP1* (*bdp1*-Δ355-372), which by itself is temperature sensitive, is synthetically lethal when combined with *PCF1-1* (15). Similarly, the more stringent requirements for both Brf1 and Bdp1 in TFIIIC-dependent complex assembly versus TBP-directed (TFIIIC-independent) assembly have been interpreted to reflect a need for interactions that reposition TFIIIC in order to allow TFIIIB complex assembly and other downstream steps in transcription to proceed (21, 25). Finally, mutations at amino acid 190 that fail to express the *sup9-e A19-supS1* suppressor (and surely lack stabilizing intramolecular interactions proposed above) have no obvious growth defects on complete medium (Fig. 2). Cell growth under normal conditions, it seems, is not limited by the functional consequences of mutations at this site. In contrast, the ability to grow on selective medium requiring the expression of the *supS1* suppressor is limited by the rate of transcription complex assembly stemming from the *sup9-e A19* promoter defect. Mutations at amino acid 190 that increase the lifetime of the alternative, higher-affinity conformer are therefore able to increase the rate of complex assembly and transcription of the mutant promoter.

In agreement with earlier observations (33), we found that wild-type TFIIIC-DNA complexes could not be quantitatively converted into Brf1-containing complexes in the absence of TBP and Bdp1 (Fig. 3 and 5). This reaction appeared to reach saturation at about 80% conversion whereas it could be driven to completion with mutant TFIIIC (Fig. 6). A simple explanation for this result, consistent with the apparent Brf1 binding affinities (Fig. 6), is that wild-type Brf1-TFIIIC-DNA complexes may be less stable relative to complexes containing *PCF1-1* TFIIIC and thus may dissociate during gel electrophoresis. However, our experiments were unable to detect in-gel dissociation of these complexes (Fig. 4). Nonetheless, it remains possible that about 20% of the wild-type Brf1-TFIIIC-DNA complexes may dissociate prior to entry into the gel. Alternatively, a conformationally distinct TFIIIC fraction may exist in which the Brf1 binding site is blocked (proposed initially in reference 33). Further evaluation of this behavior will require the development of new assays in this system.

Both halves of Brf1 interact with TFIIIC-DNA (21), and two-hybrid experiments indicate that the TFIIB-like half of Brf1 interacts with the amino terminus (Nt-TPR1) of TFIIIC131 (3). However, the regions of Brf1 that interact with the two independent binding sites in TFIIIC131 (Nt-TPR5 and TPR6 to TPR9) have not been defined biochemically. Moreover, it is not clear how Brf1 interacts with the large Nt-TPR9 fragment. In this regard, it is interesting that the apparent Brf1 binding constant for the mutant Nt-TPR9 fragment (192 ± 30 nM [Table 1]) is identical within experimental error to that for TPR6 to TPR9 (177 ± 27 nM [32]). Thus, the *PCF1-1* mutation may relieve autoinhibition of Brf1 binding to TPR6 to TPR9. Of course, more complex interactions could also account for the data. In any event, it is certain that the high-affinity Brf1 binding site in Nt-TPR5 remains largely, if not entirely, inaccessible in the mutant Nt-TPR9 fragment. As noted previously for the wild-type fragment (32), this implies that Brf1 may bind sequentially to the two sites in TFIIIC131, within the context of TFIIIC. Given the apparent need for repositioning of TFIIIC131 in order to allow Bdp1 binding (21, 25), we suggest that the interactions between Brf1 and TFIIIC131 may be modified (e.g., extended or exchanged) at this stage in the assembly process.

ACKNOWLEDGMENTS

We thank Akira Ishiguro and E. Peter Geiduschek for communicating their results prior to publication.

This work was supported by National Institutes of Health grant GM42728.

REFERENCES

1. **Abe, Y., T. Shodai, T. Muto, K. Mihara, H. Torii, S. Nishikawa, T. Endo, and D. Kohda.** 2000. Structural basis of presequence recognition by the mitochondrial protein import receptor Tom20. Cell **100:**551–560.
2. **Bartholomew, B., G. A. Kassavetis, and E. P. Geiduschek.** 1991. Two components of *Saccharomyces cerevisiae* transcription factor IIIB (TFIIIB) are stereospecifically located upstream of a tRNA gene and interact with the second-largest subunit of TFIIIC. Mol. Cell. Biol. **11:**5181–5189.
3. **Chaussivert, N., C. Conesa, S. Shaaban, and A. Sentenac.** 1995. Complex interactions between yeast TFIIIB and TFIIIC. J. Biol. Chem. **270:**15353–15358.
4. **Cloutier, T. E., M. D. Librizzi, A. K. Mollah, M. Brenowitz, and I. M. Willis.** 2001. Kinetic trapping of DNA by transcription factor IIIB. Proc. Natl. Acad. Sci. USA **98:**9581–9586.
5. **Das, A. K., P. W. Cohen, and D. Barford.** 1998. The structure of the tetratricopeptide repeats of protein phosphatase 5: implications for TPR-mediated protein-protein interactions. EMBO J. **17:**1192–1199.
6. **Dumay, H., L. Rubbi, A. Sentenac, and C. Marck.** 1999. Interaction between yeast RNA polymerase III and transcription factor TFIIIC via ABC10α and τ131 subunits. J. Biol. Chem. **274:**33462–33468.
7. **Dumay-Odelot, H., J. Acker, R. Arrebola, A. Sentenac, and C. Marck.** 2002. Multiple roles of the τ131 subunit of yeast transcription factor IIIC (TFIIIC) in TFIIIB assembly. Mol. Cell. Biol. **22:**298–308.
8. **Durfee, T., K. Becherer, P. L. Chen, S. H. Yeh, Y. Yang, A. E. Kilburn, W. H. Lee, and S. J. Elledge.** 1993. The retinoblastoma protein associates with the protein phosphatase type 1 catalytic subunit. Genes Dev. **7:**555–569.
9. **Gatto, G. J., Jr., B. V. Geisbrecht, S. J. Gould, and J. M. Berg.** 2000. Peroxisomal targeting signal-1 recognition by the TPR domains of human PEX5. Nat. Struct. Biol. **7:**1091–1095.
10. **Geiduschek, E. P., and G. A. Kassavetis.** 2001. The RNA polymerase III transcription apparatus. J. Mol. Biol. **310:**1–26.
11. **Grove, A., G. A. Kassavetis, T. E. Johnson, and E. P. Geiduschek.** 1999. The RNA polymerase III-recruiting factor TFIIIB induces a DNA bend between the TATA box and the transcriptional start site. J. Mol. Biol. **285:**1429–1440.

12. **Guex, N., and M. C. Peitsch.** 1997. SWISS-MODEL and the Swiss-Pdb-Viewer: an environment for comparative protein modeling. Electrophoresis **18:**2714–2723.
13. **Huang, Y., and R. J. Maraia.** 2001. Comparison of the RNA polymerase III transcription machinery in *Schizosaccharomyces pombe*, *Saccharomyces cerevisiae* and human. Nucleic Acids Res. **29:**2675–2690.
14. **Huet, J., C. Conesa, C. Carles, and A. Sentenac.** 1997. A cryptic DNA binding domain at the COOH terminus of TFIIIB70 affects formation, stability, and function of preinitiation complexes. J. Biol. Chem. **272:**18341–18349.
15. **Ishiguro, A., G. A. Kassavetis, and E. P. Geiduschek.** 2002. Essential roles of Bdp1, a subunit of RNA polymerase III initiation factor TFIIIB, in transcription and tRNA processing. Mol. Cell. Biol. **22:**3264–3275.
16. **Joazeiro, C. A., G. A. Kassavetis, and E. P. Geiduschek.** 1996. Alternative outcomes in assembly of promoter complexes: the roles of TBP and a flexible linker in placing TFIIIB on tRNA genes. Genes Dev. **10:**725–739.
17. **Kang, H., S. L. Sayner, K. L. Gross, L. C. Russell, and M. Chinkers.** 2001. Identification of amino acids in the tetratricopeptide repeat and C-terminal domains of protein phosphatase 5 involved in autoinhibition and lipid activation. Biochemistry **40:**10485–10490.
18. **Kassavetis, G. A., B. Bartholomew, J. A. Blanco, T. E. Johnson, and E. P. Geiduschek.** 1991. Two essential components of the *Saccharomyces cerevisiae* transcription factor TFIIIB: transcription and DNA-binding properties. Proc. Natl. Acad. Sci. USA **88:**7308–7312.
19. **Kassavetis, G. A., B. R. Braun, L. H. Nguyen, and E. P. Geiduschek.** 1990. *S. cerevisiae* TFIIIB is the transcription initiation factor proper of RNA polymerase III, while TFIIIA and TFIIIC are assembly factors. Cell **60:**235–245.
20. **Kassavetis, G. A., C. A. Joazeiro, M. Pisano, E. P. Geiduschek, T. Colbert, S. Hahn, and J. A. Blanco.** 1992. The role of the TATA-binding protein in the assembly and function of the multisubunit yeast RNA polymerase III transcription factor, TFIIIB. Cell **71:**1055–1064.
21. **Kassavetis, G. A., A. Kumar, E. Ramirez, and E. P. Geiduschek.** 1998. Functional and structural organization of Brf, the TFIIB-related component of the RNA polymerase III transcription initiation complex. Mol. Cell. Biol. **18:**5587–5599.
22. **Kassavetis, G. A., G. A. Letts, and E. P. Geiduschek.** 2001. The RNA polymerase III transcription initiation factor TFIIIB participates in two steps of promoter opening. EMBO J. **20:**2823–2834.
23. **Kassavetis, G. A., D. L. Riggs, R. Negri, L. H. Nguyen, and E. P. Geiduschek.** 1989. Transcription factor IIIB generates extended DNA interactions in RNA polymerase III transcription complexes on tRNA genes. Mol. Cell. Biol. **9:**2551–2566.
24. **Khoo, B., B. Brophy, and S. P. Jackson.** 1994. Conserved functional domains of the RNA polymerase III general transcription factor BRF. Genes Dev. **8:**2879–2890.
25. **Kumar, A., G. A. Kassavetis, E. P. Geiduschek, M. Hambalko, and C. J. Brent.** 1997. Functional dissection of the B″ component of RNA polymerase III transcription factor IIIB: a scaffolding protein with multiple roles in assembly and initiation of transcription. Mol. Cell. Biol. **17:**1868–1880.
26. **Lapouge, K., J. S. Smith, A. P. Walker, J. S. Gamblin, J. S. Smerdon, and K. Rittinger.** 2000. Structure of the TPR domain of p67phox in complex with Rac.GTP. Mol. Cell **6:**899–907.
27. **Leveillard, T., G. A. Kassavetis, and E. P. Geiduschek.** 1991. *Saccharomyces cerevisiae* transcription factors IIIB and IIIC bend the DNA of a tRNA(Gln) gene. J. Biol. Chem. **266:**5162–5168.
28. **Librizzi, M. D., R. D. Moir, M. Brenowitz, and I. M. Willis.** 1996. Expression and purification of the RNA polymerase III transcription specificity factor IIIB70 from *Saccharomyces cerevisiae* and its cooperative binding with TATA-binding protein. J. Biol. Chem. **271:**32695–32701.
29. **Lopez-de-Leon, A., M. Librizzi, K. Puglia, and I. M. Willis.** 1992. PCF4 encodes an RNA polymerase III transcription factor with homology to TFIIB. Cell **71:**211–220.
30. **Marck, C., O. Lefebvre, C. Carles, M. Riva, N. Chaussivert, A. Ruet, and A. Sentenac.** 1993. The TFIIIB-assembling subunit of yeast transcription factor TFIIIC has both tetratricopeptide repeats and basic helix-loop-helix motifs. Proc. Natl. Acad. Sci. USA **90:**4027–4031.
31. **Moir, R. D., K. V. Puglia, and I. M. Willis.** 2000. Interactions between the tetratricopeptide repeat-containing transcription factor TFIIIC131 and its ligand, TFIIIB70. Evidence for a conformational change in the complex. J. Biol. Chem. **275:**26591–26598.
32. **Moir, R. D., K. V. Puglia, and I. M. Willis.** 2002. Autoinhibition of TFIIIB70 binding by the tetratricopeptide repeat-containing subunit of TFIIIC. J. Biol. Chem. **277:**694–701.
33. **Moir, R. D., I. Sethy-Coraci, K. Puglia, M. D. Librizzi, and I. M. Willis.** 1997. A tetratricopeptide repeat mutation in yeast transcription factor IIIC131 (TFIIIC131) facilitates recruitment of TFIIB-related factor TFIIIB70. Mol. Cell. Biol. **17:**7119–7125.
34. **Persinger, J., S. M. Sengupta, and B. Bartholomew.** 1999. Spatial organization of the core region of yeast TFIIIB-DNA complexes. Mol. Cell. Biol. **19:**5218–5234.
35. **Rameau, G., K. Puglia, A. Crowe, I. Sethy, and I. Willis.** 1994. A mutation in the second largest subunit of TFIIIC increases a rate-limiting step in transcription by RNA polymerase III. Mol. Cell. Biol. **14:**822–830.
36. **Ruth, J., C. Conesa, G. Dieci, O. Lefebvre, A. Dusterhoft, S. Ottonello, and A. Sentenac.** 1996. A suppressor of mutations in the class III transcription system encodes a component of yeast TFIIIB. EMBO J. **15:**1941–1949.
37. **Scheufler, C., A. Brinker, G. Bourenkov, S. Pegoraro, L. Moroder, H. Bartunik, F. U. Hartl, and I. Moarefi.** 2000. Structure of TPR domain-peptide complexes: critical elements in the assembly of the Hsp70-Hsp90 multichaperone machine. Cell **101:**199–210.
38. **Sethy-Coraci, I., R. D. Moir, A. Lopez-de-Leon, and I. M. Willis.** 1998. A differential response of wild type and mutant promoters to TFIIIB70 overexpression in vivo and in vitro. Nucleic Acids Res. **26:**2344–2352.
39. **Taylor, P., J. Dornan, A. Carrello, R. F. Minchin, T. Ratajczak, and M. D. Walkinshaw.** 2001. Two structures of cyclophilin 40. folding and fidelity in the tpr domains. Structure (Cambridge) **9:**431–438.
40. **White, R. J.** 1998. RNA polymerase III transcription. Springer-Verlag, New York, N.Y.
41. **Willis, I., A. Oksman, and A. Lopez-de-Leon.** 1992. The PCF1–1 mutation increases the activity of the transcription factor (TF) IIIB fraction from *Saccharomyces cerevisiae*. Nucleic Acids Res. **20:**3725–3730.
42. **Willis, I., P. Schmidt, and D. Soll.** 1989. A selection for mutants of the RNA polymerase III transcription apparatus: PCF1 stimulates transcription of tRNA and 5S RNA genes. EMBO J. **8:**4281–4288.